



ON TRIDIMENSIONAL RIP CURRENT MODELING

PATRICK MARCHESIELLO⁽¹⁾, RACHID BENSHILA⁽²⁾, RAFAEL ALMAR⁽³⁾, YUSUKE UCHIYAMA⁽⁴⁾, JAMES MCWILLIAMS⁽⁵⁾ & ALEXANDER SHCHEPETKIN⁽⁶⁾

⁽¹⁾ *Institute of Research for Development, Toulouse, France,
Patrick.Marchesiello@ird.fr*

⁽²⁾ *Centre National de la Recherche Scientifique, Toulouse, France
Rachid.Benshila@legos-obs-mip.fr*

⁽³⁾ *Institute of Research for Development, Toulouse, France,
Rafael.Almar@ird.fr*

⁽⁴⁾ *Kobe University, Kobe, Japan,
uchiyama@harbor.kobe-u.ac.jp*

⁽⁵⁾ *University of California at Los Angeles, Los Angeles, California
jcm@atmos.ucla.edu*

⁽⁶⁾ *University of California at Los Angeles, Los Angeles, California,
alex@atmos.ucla.edu*

ABSTRACT

Low-frequency variability generated by lateral shear instabilities of the coastal circulation may promote stirring and mixing of coastal waters. The question remains open to whether tridimensional transient processes are important for the generation of these instabilities and for surf-shelf exchanges in general. An innovative modeling system with tridimensional wave-current interactions (McWilliams et al., 2004) was designed to investigate transient nearshore currents and interaction between nearshore and innershelf circulations. We present here some validation of rip current modeling in the French coastal zone (Bruneau et al., 2011) using in-situ and remote video sensing. We then proceed to show the benefits of 3D versus 2D modeling for the simulation of mean rip currents and their low-frequency variability. It is concluded that tridimensional nearshore models may provide a valuable and cost-effective alternative to more usual 2D approaches, which miss the vertical flow structure and its nonlinear interaction with the 2D flow.

Keywords: Rip; Video; Modeling; Tridimensional; Biscarrosse.

1. INTRODUCTION

Rip currents are narrow, seaward currents that extend from the inner surf zone out through the line of breaking waves. Rip currents are usually long (100 m), narrow (10 m) and intense jet flow (reaching 1-2 m/s). They appear to span the entire water column in the shallow breaking zone but they remain confined near the surface as they flow past the breaking zone into deeper water, showing strong vertical shear. Understanding and predicting the complex tridimensional dynamics of rip currents remain a relevant scientific challenge because they play a key role on the beach and surf zone morphodynamics, on the dispersion of material across the surf zone and are a major hazard to swimmers [see MacMahan et al., 2006, for a review].

Despite substantial evidence of tridimensional effects, most modeling studies of rip currents are performed using depth-integrated shallow water equations. Bruneau et al. (2011) used this class of model (MARS coupled with SWAN) to study the Aquitanian coast of France. In June 2007 an intense 5-day field experiment was conducted at the mesotidal - macrotidal wave - dominated Biscarrosse Beach on a well - developed bar and rip morphology. Previous analysis of the field data exposed the main characteristics of a tide - modulated rip current driven by low - to high - energy shore - normal waves (Bruneau et al., 2009a). The model was able to reproduce some of the

characteristics of the rip currents but discrepancies with observations at the rip neck were evidenced, particularly in the cross-shore component.

In a parallel study, Bruneau et al. (2009b) showed occurrence of rip current variability, referred to as Very Low Frequency motions (VLF), in the rip neck where VLF pulsations were most intense (reaching 1m/s on time scales of 10 to 30 minutes). The model was specifically tuned (reduced viscosity compared to the otherwise more realistic control simulation) to develop shear instabilities consistent with the analytical solution of Haller and Dalrymple (2001).

In this paper, we extend on the work of Bruneau et al. (2009b and 2011) to show that tridimensional wave-current interactions cannot be dismissed in the study of rip current dynamics and that their expression is evident both in their persistent structure and instability behavior.

2. METHODS

2.1 Video monitoring

A main limitation for understanding nearshore processes is lack of appropriate observation, particularly in tropical environments. Traditional in-situ measurement techniques can provide high sampling rates and a direct estimation of many parameters but with coarse spatial resolution that often miss complex dynamical interactions.

Additionally, instruments must be deployed in high-energy and sometimes hazardous environments (wave-breaking, strong currents), endangering not only the instruments, but also the personnel involved. As an alternative, remote sensing techniques can provide synoptic coverage over large areas with a wide range of temporal and spatial resolutions.

The innovative video imaging technique (Holman and Haller, 2013) is particularly suited to coastal observation: low cost and easy to deploy. It is also considered as a non-disruptive observation technique for nearshore research. A video system was deployed at Biscarosse beach in 2007 and new inversion methods (Almar et al., 2009; see Fig. 1) were used to provide a remote estimation of the complete nearshore system, i.e., hydrodynamics (wave height, period, celerity, direction, wavelength, water level, current) and morphodynamics (shoreline, sub- and intertidal bathymetry) continuously and over long-term periods and large areas (approximate 2x1 km).

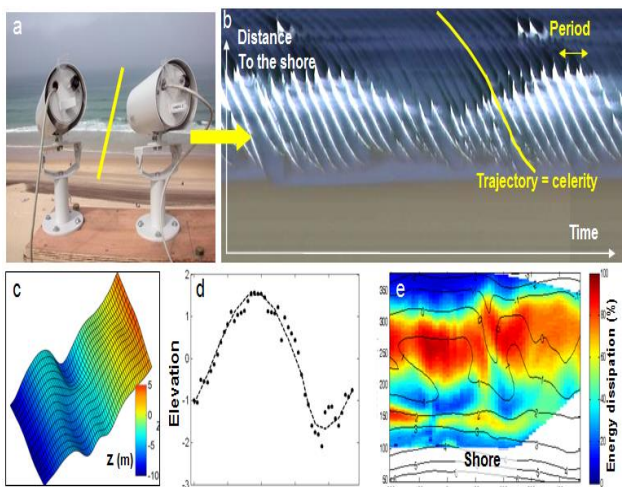


Figure 1. Coastal video monitoring: description of applications; (a) 5-camera system for Biscarosse (France); (b) Spatial-temporal post-processed image showing wave dynamics. The image is generated from the high frequency acquisition of a cross-shore array of pixels. (c) Bathymetric inversion from wave dispersion. (d) Video-estimated water level. (e) 2D field of wave-breaking dissipation.

2.2 The model: ROMS

The objective of the paper is to assess the benefit of tridimensional coastal models. An innovative modeling approach for 3D wave-current interactions (McWilliams et al., 2004) was implemented in the Regional Oceanic Modeling System (ROMS; Shchepetkin and McWilliams, 2005) by Uchiyama et al. (2010) and used for idealized rip current studies (Weir et al., 2011). An upgraded version of this implementation is proposed here based on the AGRIF version of ROMS (Penven et al., 2006; Debreu et al., 2012). It allows additional capabilities such as nesting and wetting/drying (Warner et al., 2013), the latter being crucial to the meso- macro-tidal environment of Biscarosse beach.

ROMS is a hydrostatic, incompressible, free-surface and terrain-following coordinate model with non-conservative forcing, diffusion, and bottom drag. It uses baroclinic-barotropic mode splitting, with explicit fast time-stepping and subsequent conservative averaging of barotropic variables. The discretization is with high-order finite differences that provide both accurate and cost-effective solutions. Open boundary conditions use a combination of

characteristic methods (barotropic part) and radiation (baroclinic part) with Newtonian and viscous damping (Marchesiello et al., 2001).

The interaction of surface gravity waves and currents is implemented in ROMS through vortex-force (VF) formalism. Eulerian wave-averaged current equations for mass, momentum, and tracers are included based on an asymptotic theory by McWilliams et al. (2004) plus non-conservative wave effects due to wave breaking, associated surface roller waves, bottom streaming, and wave-enhanced vertical mixing and bottom drag. The nonlinear parameterization of Soulzby (1995) for wave-enhanced bottom drag is particularly relevant to the present case with strong tidal flow. All parameterizations are described in details in Uchiyama et al., 2010 (see also Blaas et al., 2007 for bottom drag formulation).

The currents are coupled with a ray-theory spectrum-peak propagation and refraction model (WKB model) that includes the effect of currents on waves and dissipation due to shoaling-induced wave breaking. The system is thus fully coupled within a unique executable code that is easy to handle.

The advantage of the vortex-force over radiation-stress formalism is to cleanly decouple conservative and non-conservative effects on currents and, within the conservative effects, the vortex force and Bernoulli head components. The non-conservative components (acceleration/dissipation) are those that require parameterization and are thus responsible for the largest uncertainties in our model formulation. Clear identification of these terms is thus of primary interest. Another advantage of the VF formalism is numerical since it requires taking one less derivative in space and thus produces fewer numerical approximations (Weir et al., 2011).

The coupled system is applied to the nearshore surf zone during the 2007 Biscarosse field measurement campaign (see Bathymetry in Figure 2). Offshore measurements of tidal elevation, wave height and winds are used to force the model for 5 days from the 13th to the 17th of June 2007. The horizontal resolution is 10m; there is 20 vertical sigma levels equally spaced. The horizontal viscosity coefficient is given by the flow- and resolution-dependent Smagorinsky formulation (between 0 and 2 m²/s). The baroclinic time step is 2 seconds and 30 barotropic sub-steps are performed every baroclinic step. The cost of 3D computations is thus moderate and the full 3D model is only marginally more expensive than the 2D part.

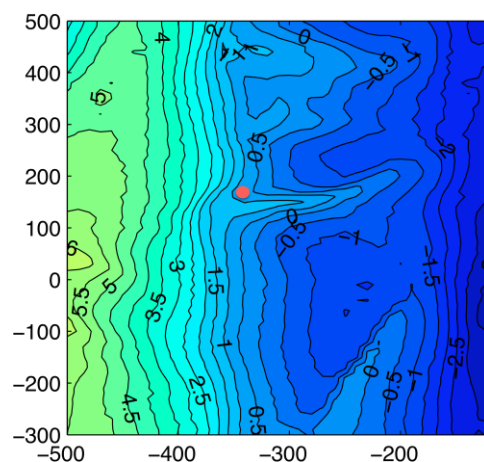


Figure 2. Model domain and interpolated bathymetry. The orange dot shows the measurement station S4 at the rip neck where model-data comparisons are presented.

In the following, the model results are compared to observations and tridimensional effects are investigated with emphasis on the vertical profile of cross-shore currents.

3. CALIBRATION AND VALIDATION

3.1 Calibration with video data

There is still no consensus on many parameterizations: wave-driven flow acceleration and turbulent mixing, contribution of the breaking wave roller, bottom friction and boundary layer streaming (e.g., Uchiyama et al., 2010). In particular, the parameterization of breaking wave dissipation is crucial to nearshore dynamics but is generally guided by scarce data.

One of the novelties of our method lies in the tuning of breaking wave dissipation (including roller dissipation) in the wave model by direct comparison with 2D video imagery (Figure 3). The wave model uses the parameterization of Church and Thornton (1993), which has the particularity of producing more shoaling of the incoming wave before breaking and thus more intense breaking than other choices (Weir et al., 2011). It relies on two empirical constants: the breaking wave parameter γ_b (wave height-to-depth ratio) and B_b the percentage of the wave face that is broken. Values of 0.3 and 1.3, respectively, provide the best fit to data. As opposed to Bruneau et al. (2011), there is no need here to add a time dependence on γ_b as the fit to data appears valid for both low- and high-energy conditions. The fraction α_r of breaking waves converted into rollers is taken as 0.5 and reveals only little sensitivity.

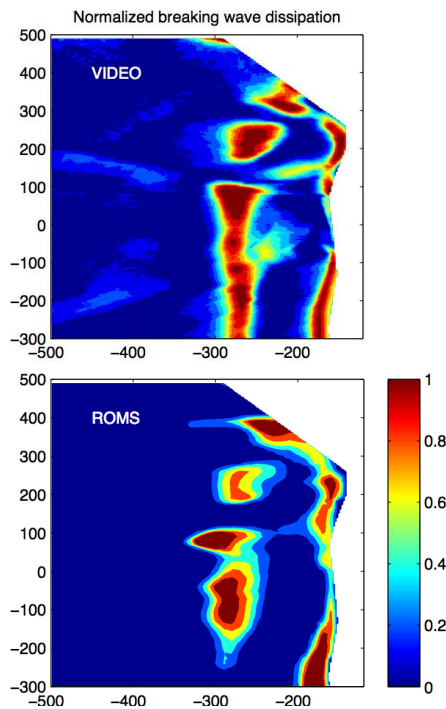


Figure 3. Normalized wave-breaking dissipation from the video data and from ROMS after calibration.

3.2 Validation with in-situ data

Figure 4 shows a model-data comparison for wave height and cross-shore currents at station S4 located at the rip

neck (see Figure 2). The observation shows a strong increase of wave height on the 15th of June due to offshore forcing but strongly modulated by large tides (with range of close to 4 m) that shift back and forth the cross-shore position of the breaking line. High-energy conditions from June 15th lead to strong offshore-directed rip currents in excess of 75 cm/s. The model is able to reproduce the evolution of both wave height and currents. The wave model fit is quite remarkable during high-energy conditions, validating our assumption that nearshore waves in this experiment are well described by ray equations driving a monochromatic wave with the root-mean-square wave height and frequency corresponding to the spectral peak. There is an equally remarkable fit of simulated currents with data, in contrast with the 2D simulations shown by Bruneau et al. (2011).

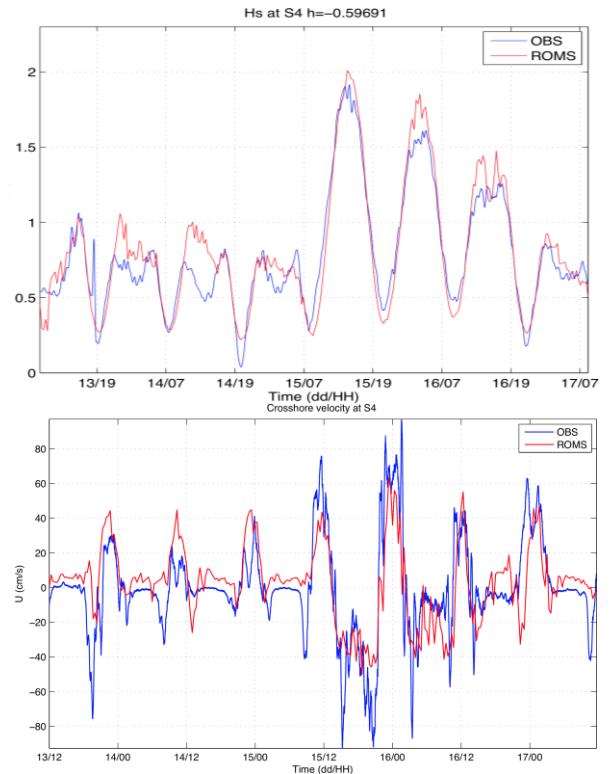


Figure 4. Model-data comparison at station S4 for wave height (top) and cross-shore currents (bottom).

4. ANALYSIS AND SENSITIVITY

4.1 Comparing 2D and 3D solutions

To analyze the extent of errors related to the 2D shallow water hypothesis, we now compare our standard solution with a 2D version. In this case the barotropic mode is advanced alone. Note that the barotropic (depth-averaged) flow of the 2D model is different from that of the 3D model because in the latter it receives contribution from the baroclinic flow, in particular the baroclinic contribution to nonlinear terms (Reynolds stresses of type $\overline{uu} - uu$, where the overbar denotes the depth average). For the bottom drag due to currents¹, we use an equivalent formulation to the 3D case. Assuming that in shallow water the logarithmic layer extends all the way to

¹ The total bottom drag law is a nonlinear combination of current and wave contributions according to Soulsby (1995). The bottom stress due to waves has no dependence on the vertical grid.

the surface, we can integrate the velocity profile to obtain a 2D drag coefficient of the form:

$$C_D = \frac{\kappa^2}{\left[\ln(H/z_0) - 1\right]^2} \quad [1]$$

where H is total depth, z_0 is bottom roughness and κ is Von Karman constant. This formulation ensures that the 2D bottom stress equals that of the 3D model for the same barotropic flow (again assuming logarithmic velocity profiles).

Figure 5 shows a comparison of the barotropic components of ROMS in its shallow water and 3D versions (ROMS2D and ROMS3D, respectively). It appears that ROMS2D strongly underestimates the cross-shore flow during high-energy conditions, especially the rip currents (negative values at time 150-170). This result is also very comparable to that of the 2D model used in Bruneau et al. (2011). Interestingly, the barotropic mode of the 3D model shows larger velocities implying a significant role played by the baroclinic contribution to barotropic nonlinear terms. This result is quite important as it shows that the total flow cannot simply be addressed by linear combination of a depth-averaged model and a vertical profile technique, a common approach in morphological models (e.g., De Vriend and Stive, 1987).

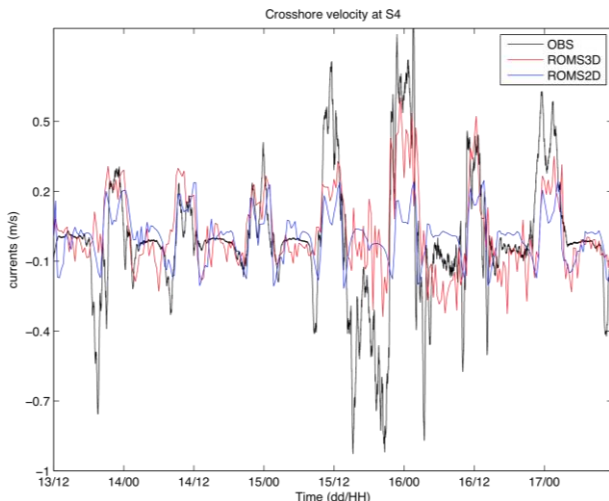


Figure 5. Depth-averaged component of cross-shore velocity in ROMS2D and ROMS3D compared with data. See Figure 4 for total model cross-shore currents.

The vertical structure of the 3D flow has several dependencies. First, it is strongly affected by the profile distribution function of breaking and roller acceleration. The best fit to data is obtained with a surface-intensified breaking force, consistent with Uchiyama et al. (2010). On the other end, the wave-induced mixing scale is larger than breaking acceleration scale and requires a smoother vertical distribution function (again as in Uchiyama et al., 2010). We also find that the choice of bottom friction formulation is less sensitive than breaking acceleration for representing the proper flow structure. Finally, the currents' vertical structure is significantly shaped by the vertical component of vortex force.

5. RIP CURRENT INSTABILITIES

Turbulence generated by the coastal circulation is probably responsible for large mixing and transport in coastal waters (Brocchini et al., 2004). Weir et al. (2011) show that the feedback effect of currents on waves reduces the cross-shore extension of turbulence but in the

same time enhances nearshore eddy energy. In particular, rip currents contain energetic low-frequency oscillations, which does not require low-frequency wave forcing.

5.1 Background

Haller and Darlymple (2001) developed an analytic model to study the linear spatial stability of a rip current² and show that low-frequency oscillations can be explained by shear-flow (vortical) instabilities. In absence of friction and bottom slope, the results are consistent with those of the classical Bickley jet³ (Bickley, 1939). The fastest growing sinuous mode of Haller and Darlymple (2001) produces jet meandering with non-dimensional wavenumber $k^*=0.639$ and frequency $\sigma^*=0.255$, related to actual wavenumber k_0 and frequency σ_0 by a length-scale and vorticity scale respectively. The oscillations period and wavelength are given by:

$$T_0 = \frac{2\pi}{\sigma_0} = \frac{2\pi l}{\sigma^* U_{\max}}$$

$$L_0 = \frac{2\pi}{k_0} = \frac{2\pi l}{k^*}$$

Here, U_{\max} is the maximum jet velocity and l its half-width length-scale. It means that the oscillation frequency of a rip current is closely controlled by the magnitude of its vorticity, a result supported by laboratory experiments (Kennedy and Zhang, 2008). With 0.5 m/s and 20m respectively, we get a time-scale of about 15 min (and wavelength of about 200m). According to this scaling, the peak period for weaker and wider jets can increase to order 100 min. In Haller and Darlymple (2001), viscosity, bottom friction and bottom slope play a large role in controlling vorticity (through offshore jet spreading) and thus the instability process. In general, friction has a strong stabilizing effect and would increase the period of unstable oscillations. The bottom slope has a similar effect. Though vortex stretching tends to reduce jet spreading (as opposed to bottom friction), continuity of the depth-averaged flow has a stronger effect in reducing the jet speed. In the tridimensional problem, surface trapping past the surf zone would be less sensitive to both vortex stretching and continuity effects but with uncertain outcome on the overall contribution of bottom slope to jet vorticity.

Kennedy and Zhang (2008) developed a stability analysis for a more complex configuration with wave-current interactions that required a numerical solver (for the eigenvalue problem). They mostly confirmed the results of Haller and Darlymple (2001) and clarified the characteristics of the two types of shear-flow instability: sinuous and varicose. The former and dominant one is vorticity driven and occurs for strong rip currents (0.5 m/s) and the second for weaker rip currents has its strongest bulging signature shoreward of the bar. In Kennedy and Zhang (2008), oscillatory periods of unstable jet modes for various conditions (particularly friction) varied between around 8 and 14 min. Their peak periods are a smaller than in Haller and Darlymple (2001) because

² Exponential growth of normal modes along the jet axis is considered with real frequency and complex wave number.

³ The Bickley jet is a parallel flow with profile function $\text{sech}^2=1/\cosh^2$ about the centerline and has inflection points (change of sign of vorticity gradients) satisfying the Rayleigh criterion for shear-flow instability. It produces two types of unstable modes: the sinuous and varicose modes.

they consider a different maximum vorticity scale taken at the feeder zone. Interestingly, the coarsening of grid resolution in these experiments has a similar effect to friction, since jet vorticity is underestimated in this case as well. Kennedy and Zhang (2008) also expose a wave-current-type instability at higher periods (beyond 30mn) but only for small wave heights. Wave-current modes are due to a feedback mechanism between the rip current and longshore pressure gradients associated with flow-driven wave height variations. They grow slowly and may impose a slow pulsation to the rip current (Haas et al., 2003) while they develop downstream of the jet, much as a convective instability. However, a major effect of wave-current interaction (for all wave height) is to reduce the intensity of rip currents, their offshore extension and shear instability (Haas et al., 2003; Weir et al., 2011).

5.1 Biscarosse

Figure 6 shows a snapshot of rip current flow advecting a passive tracer. The general pattern shows a rip flow biased towards the south and a strong cyclonic recirculation cell, very similar to that of Haas et al. (2003). It also suggests the presence of turbulence, i.e., meandering and offshore-developing instability with a mushroom-shaped pattern detaching from the rip recirculation cell. The maximum vorticity within the rip current is larger than 0.05 s^{-1} , which is on the order of the vorticity scaling used as example above.

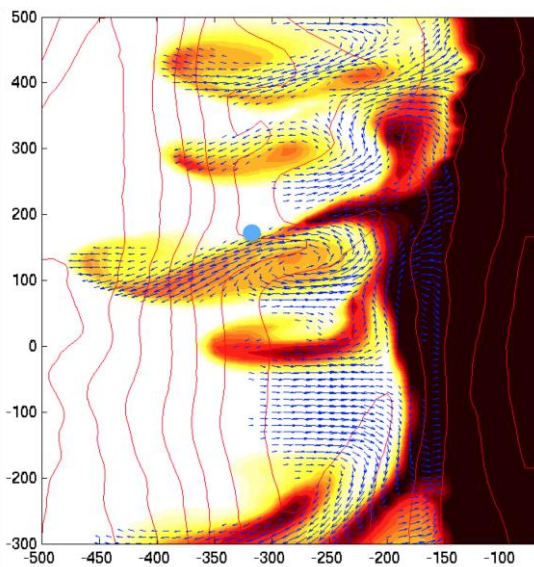


Figure 6. Snapshot of surface flow (vectors) advecting a passive tracer initially released in 1-m depth.

Bruneau et al (2009b) noted VLF oscillations in Biscarosse time-series with periods of 10-30 min. This is a considerably longer period than most subharmonic wave energy but is well within the range of possible shear instability (Kennedy and Zhang, 2008). The problem is complicated by the fact that the frequency spectrum from this data shows energy at all frequencies due to the wide range of conditions during the 5-day campaign (Figure 8). However, low-pass filtering of the data indicates occurrence of VLF oscillations that are correlated with the presence of rip currents (Figure 7). This observation is consistent with mean-eddy conversion associated with flow instability rather than low-frequency wave forcing.

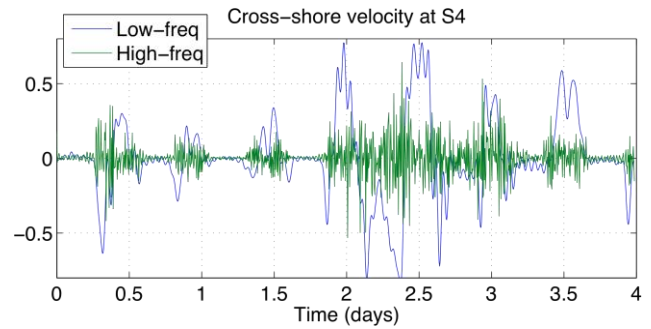


Figure 7. Observed time series of cross-shore velocity at station S4 during the June 2007 campaign (starting on the 13th at noon). The blue curve is low-pass filtered at 1 hour and the green curve is high-pass filtered at 30 min.

In the model, the frequency of variability associated with VLF motions is consistent with the data although the amplitude of oscillations is lower (Figure 7). It should be noted that the time interval of model wave forcing is 20 min; therefore all scales below 40 min are intrinsic in the model. Part of the missing energy may thus be related to forcing conditions. Another part may be due to the resolution of fine vorticity scales. Some experiments with increased resolution (5m) or decreased viscosity (Smagorinsky coefficient reduced by half) have enhanced VLF energy.

To better extract and analyze the intrinsic part of variability in the simulation, we designed a stationary experiment using the low-energy conditions of June 2007 as a persistent forcing. The result compares well with the spectrum of unstable normal modes given by Haller and Darlymple (2001; see their Figure 19). There is a range of VLF oscillations between 10-30 min in agreement with the scaling given above from analytical estimations. However, a range of energetic but slower oscillations (30-50 min) is also present that is either due to wave-current interactions or nonlinear growth of unstable perturbations. Interestingly, increasing model viscosity removes the highest frequency motions but leaves out part of the oscillations around 50 min.

VLF oscillations are nearly absent from the 2D simulations. In Figure 7, all periods of oscillations below about 50 min are considerably weaker than in the 3D model and even weaker than in the data. Consistently, Bruneau et al. (2009b) failed to capture VLF frequencies in their standard 2D simulations and significant viscosity reduction was required to generate instabilities in their case. We interpret this result as evidence that the barotropic component of 2D equations is too weak to produce much current shear that triggers instabilities.

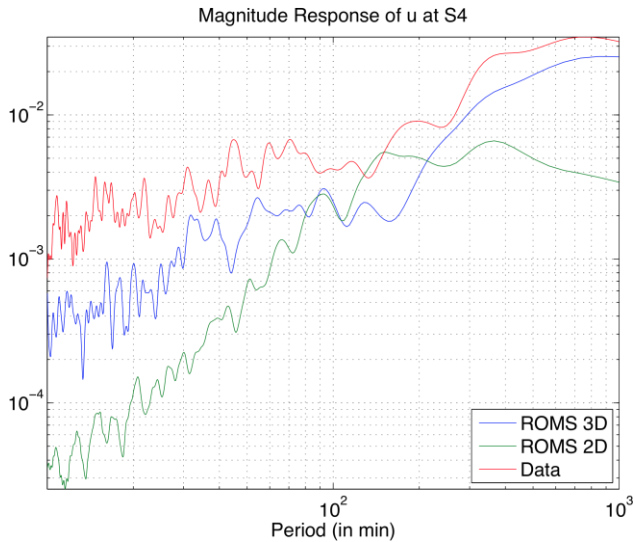


Figure 8. Frequency spectrum of cross-shore velocity at the rip neck (station S4) during the 5-day Biscarosse campaign of 2007. 2D and 3D models are compared with data.

In linear models, lateral or bottom friction increases the jet spreading of the classical planar jet solution and causes the centerline velocity to decay more rapidly. We have noted that the bottom slope acts in the same direction as friction because depth-averaged flow continuity overwhelms the effect of vortex stretching (Haller and Darlymple, 2001). Interestingly and as already predicted by Arthur (1962), this balance should be affected by tridimensionality. After rip currents leave the surf zone they tend to be confined to a layer of thickness equal to the depth at the seaward edge of the surf zone. This would have a double effect. On one hand, surface confinement should reduce bottom interaction and associated stretching effect. On the other hand, bottom friction should also decrease in the process. More importantly, a surface-intensified jet has more intense centerline velocity than its depth-averaged flow on a sloping beach (due to continuity). From our results, nonlinear interactions between baroclinic and barotropic components also appear to increase the barotropic flow. Overall, the increase of shear production from surface intensification appears to easily dominate over depth-average dynamical balance.

To localize in space the instability process, we now compute the mean-eddy conversion terms in the stationary experiment (KmKe; e.g., Marchesiello et al., 2003). Figure 8 shows KmKe together with vorticity and velocity vectors. When conversion is positive, it indicates the work of shear instability. In contrast, negative values show locations of feedback to the mean flow. The maximum instability is clearly in the feeder zone on each side of the rip center (shown by positive and negative vorticity maxima). The instability decreases offshore along the jet axis as predicted by the sinuous instability modes. However, a new strong maximum appears at the offshore branch of the re-circulation cell. This branch is characterized by surface-trapped currents in relatively deep water, where bottom friction is weaker than in the rip channel. The offshore growth of disturbances is thus less impaired by friction. It allows the offshore branch of the cell to wander offshore and sometimes create an anticyclonic circulation as in Figure 6 (and Figure 4 of Haas et al., 2003). The cyclonic recirculation cell may partly result from nonlinearities and KmKe is negative in

the maximum vorticity cell center. In addition, the circulation cell is much weaker in a simulation with increased viscosity, where no instability and VLF oscillations are present.

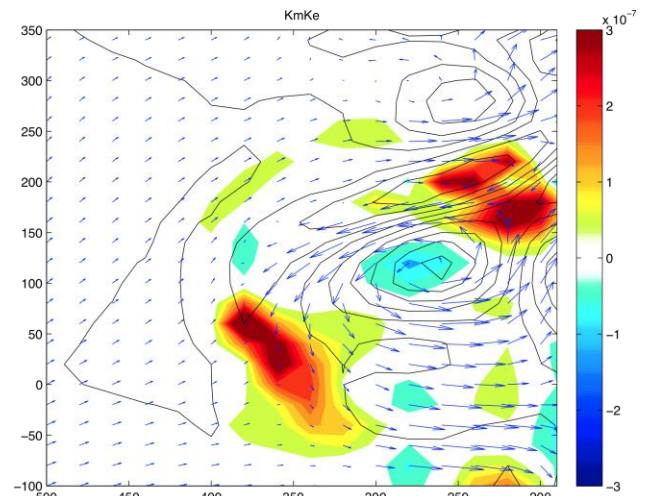


Figure 8. Mean-eddy conversion KmKe in the rip current system from a persistent 8-hour simulation of the low-energy conditions of June 2007. Vorticity contours and velocity vectors are overlaid.

There are large implications of instability problems in the ejection of surf-zone material by the rip-current system. The recirculation cell would promote retention while pulsation and filament formation would do the opposite and increase the dispersion out of the surf-zone.

6. CONCLUSIONS

We have presented some validation of tridimensional rip current modeling in the Aquitanian coastal zone using in-situ and remote video sensing. We showed the benefits of 3D versus 2D modeling for the simulation of mean rip currents and their low-frequency variability. We conclude that tridimensional nearshore models may provide a valuable and cost-effective alternative to more usual 2D approaches, which miss the vertical flow structure and its nonlinear interaction with the 2D flow.

ACKNOWLEDGMENTS

We appreciate financial support from the IRD ad CNRS. We also thank the EPOC group for providing in-situ data from the June 2007 campaign.

REFERENCES

- Almar R., Castelle B., Ruessink G., Sénéchal N., Bonneton P., Marieu V. (2009). High-frequency video observation of a double sandbar system under high-energy wave forcing. *Journal of Coastal Research*, 56, 1706-1710.
- Arthur, R. S. 1962. A note on the dynamics of rip currents. *Journal of Geophysical Research*. 67(7): 2778-2779.
- Bickley, W. 1939. The plane jet. *Phil. Mag. Ser.*, 7, 727-731.
- Blaas M., Dong C., Marchesiello P., McWilliams J.C., and Stolzenbach K.D. (2007). Sediment-transport modeling on Southern Californian shelves: A ROMS case study. *Continental Shelf Research*, 27, 832-853.
- Bruneau N., Castelle B., Bonneton P., Pedreros R., Almar R., Bonneton N., Bretel P., Parisot J.P., Senechal N.

- (2009a) Field observations of an evolving rip current on a meso-macrotidal well-developed inner bar and rip morphology, *Continental Shelf Research*, 29, 1650-1662.
- Bruneau N., Castelle B., Bonneton P., Pedreros R. (2009b) Very Low Frequency motions of a rip current system: observations and modeling, *Journal of Coastal Research*, SI 56(2), 1731-1735.
- Bruneau N., Bonneton P., Castelle B., Pedreros R. (2011) Modeling rip current circulations and vorticity in a high-energy meso-environment, *Journal of Geophysical Research*, 116, C07026.
- Debreu, L., P. Marchesiello, P. Penven, and G. Cambon, 2012. Two-way nesting in split-explicit ocean models: algorithms, implementation and validation. *Ocean Modelling*, 49-50, 1-21.
- De Vriend H.J. and Stive M.J.F. (1997). Quasi-3D modelling of nearshore currents. *Coastal Engineering*, 11, 565-601.
- Haller M.C. and Dalrymple R.A. (2001). Rip current instabilities, *J. Fluid Mech.*, 433, 161-192.
- Haas, K., Svendsen, I., Haller, M. and Zhao, Q. (2003) Quasi 3D modeling of rip current systems. *Journal of Geophysical Research*, 108(C7), 3217.
- Kennedy, A. B., and Zhang Y., 2008. The stability of wave-driven rip current circulation, *J. Geophys. Res.*, 113, C03031.
- MacMahan, J. H., E.B. Thornton, A. J. H. M. Reniers, 2006. Rip current overview. *Coastal Eng.*
- Marchesiello, P., McWilliams J.C., and Shchepetkin, A., 2001. Open boundary conditions for long-term integration of regional oceanic models. *Ocean Modelling*, 3, 1-20.
- Marchesiello P., J.C. McWilliams, and A. Shchepetkin, 2003: Equilibrium structure and dynamics of the California Current System. *Journal of Physical Oceanography*, 33, 753-783.
- McWilliams J.C., Restrepo J.M. and Lane E.M. (2004). An asymptotic theory for the interaction of waves and currents in coastal waters. *J. Fluid Mech.*, 511, 135-178.
- Penven P., L. Debreu, P. Marchesiello, and J.C. McWilliams, 2006: Evaluation and application of the ROMS 1-way embedding procedure to the central California upwelling system. *Ocean Modelling*, 12, 157-187.
- Shchepetkin, A.F., & J.C. McWilliams, 2005: The regional oceanic modeling system (ROMS): A split-explicit, free-surface, topography-following-coordinate oceanic model. *Ocean Modelling* 9, 347-404.
- Soulsby, R.L., 1995. Bed shear stresses due to combined waves and currents. In: Stive, M., Fredsøe, J., Hamm, L., Soulsby, R., Teisson, C., Winterwerp, J. (Eds.), *Advances in Coastal Morphodynamics*. Delft Hydraulics, Delft, The Netherlands, pp. 420-423.
- Uchiyama, Y., J.C. McWilliams, & A.F. Shchepetkin, 2010: Wave-current interaction in an oceanic circulation model with a vortex-force formalism: Application to the surf zone. *Ocean Modelling* 34 16-35.
- Warner J.C., Defne Z., Haas K., and Arango H.G.. 2013. A wetting and drying scheme for ROMS. *Comput. Geosci.*, 58, 54-61.
- Weir, B., Y. Uchiyama, E.M. Lane, J.M. Restrepo, & J.C. McWilliams, 2011: A vortex force analysis of the interaction of rip currents and gravity waves. *J. Geophys. Res.* 116, C05001.